

Published in IET Systems Biology
Received on 17th January 2008
Revised on 3rd June 2008
doi: 10.1049/iet-syb:20080095

Special Issue – Selected papers from the First q-bio
Conference on Cellular Information Processing



ISSN 1751-8849

Determinants of bistability in induction of the *Escherichia coli lac* operon

D.W. Dreisigmeyer¹ J. Stajic^{2,*} I. Nemenman^{2,3}
W.S. Hlavacek^{1,2} M.E. Wall^{2,3,4}

¹Theoretical Division, Los Alamos National Laboratory, Los Alamos, NM, USA

²Center for Nonlinear Studies, Los Alamos National Laboratory, Los Alamos, NM, USA

³Computer, Computational, and Statistical Sciences Division, Los Alamos National Laboratory, Los Alamos, NM, USA

⁴Bioscience Division, Los Alamos National Laboratory, Los Alamos, NM, USA

*Present address: Center for Cell Analysis and Modeling, University of Connecticut Health Center, Farmington, CT, USA

E-mail: mewall@lanl.gov

Abstract: The authors have developed a mathematical model of regulation of expression of the *Escherichia coli lac* operon, and have investigated bistability in its steady-state induction behaviour in the absence of external glucose. Numerical analysis of equations describing regulation by artificial inducers revealed two natural bistability parameters that can be used to control the range of inducer concentrations over which the model exhibits bistability. By tuning these bistability parameters, the authors found a family of biophysically reasonable systems that are consistent with an experimentally determined bistable region for induction by thio-methylgalactoside (TMG) (in Ozbudak *et al. Nature*, 2004, **427**; p. 737). To model regulation by lactose, the authors developed similar equations in which allolactose, a metabolic intermediate in lactose metabolism and a natural inducer of *lac*, is the inducer. For biophysically reasonable parameter values, these equations yield no bistability in response to induction by lactose – only systems with an unphysically small permease-dependent export effect can exhibit small amounts of bistability for limited ranges of parameter values. These results cast doubt on the relevance of bistability in the *lac* operon within the natural context of *E. coli*, and help shed light on the controversy among existing theoretical studies that address this issue. The results also motivate a deeper experimental characterisation of permease-independent transport of *lac* inducers, and suggest an experimental approach to address the relevance of bistability in the *lac* operon within the natural context of *E. coli*. The sensitivity of *lac* bistability to the type of inducer emphasises the importance of metabolism in determining the functions of genetic regulatory networks.

1 Introduction

In 1957, Novick and Weiner discovered that *Escherichia coli* can exhibit discontinuous switching in expression of the *lac* operon in response to thio-methylgalactoside (TMG), with some cells expressing a large amount of β -galactosidase (β -gal), other cells expressing a small amount and an insignificant number of cells expressing an intermediate amount [1]. Recently, this effect was further characterised using single-cell assays of fluorescence levels in a population of *E. coli* cells carrying a *lac::gfp* reporter [2].

Cells were grown overnight on sucrose in either an induced (1 mM TMG) or uninduced (no TMG) state. They were then diluted into media with defined levels of TMG and glucose; after 20 h of growth, the cells were examined under a microscope. Under many conditions, cell populations exhibited a bimodal distribution, with induced cells having over 100 times the fluorescence level of uninduced cells. The distribution was also history-dependent: at the same final level of TMG and glucose, cells with an induced history were predominantly induced, while cells with an uninduced history were predominantly

uninduced. These observations have been attributed to the existence of two steady states, that is, bistability, in the induction of *lac* in *E. coli*.

Recent modelling studies have emphasised the importance of determining whether bistability in expression of *lac* is relevant within a natural context [3–8]. This question remains open because experimental studies have focused on the response of *lac* expression to artificial inducers, such as TMG and isopropyl- β , D-thiogalactopyranoside (IPTG), rather than the natural inducer, allolactose. This difference is critical because artificial inducers (also known as gratuitous inducers) are not metabolised by the induced enzyme, whereas the natural inducer is a metabolic intermediate in lactose degradation, which is catalysed by the induced enzyme.

Savageau [3] found important differences between induction by IPTG and induction by lactose in his theoretical treatment of bistability in the *lac* operon. In Savageau's model, because production and decay of allolactose are both proportional to the β -gal concentration, bistability is forbidden. Expression of *lac* in response to lactose was therefore predicted not to exhibit bistability. This prediction agreed with the absence of steady-state bistability in an experimental study of populations of *E. coli* cells exposed to lactose, described in the Supplementary Material of Ref. [2] – in that study, only transient bimodal distributions of green fluorescence levels among cells were observed at some glucose concentrations. It was later noted that models with operon-independent decay of lactose (e.g. due to dilution by cell growth) could exhibit bistability [7]. Several studies using such models found either a bistable or graded response to lactose, depending on parameter values or external glucose levels [5–10], and, in agreement with the model of Savageau, a model of van Hoek and Hogeweg [7] was explicitly shown to exhibit no bistability in the absence of operon-independent decay of allolactose. However, these studies disagree in their assessment of whether bistability is present [5, 6, 10] or absent [7–9] in expression of *lac* among *E. coli* cells in a natural context.

In addition to predicting whether *lac* induction exhibits bistability, some studies have addressed the question of whether bistability might enhance or hinder the performance of *E. coli* cells. Both Savageau [4] and van Hoek & Hogeweg [9] found that bistability increases the time required to respond to sudden increases in environmental lactose, which can be a disadvantage in competition for nutrients. These results argue against the natural relevance of bistability in *lac* expression.

Another important question that has not yet been addressed is whether the experimental observations of bistability in Ref. [2] are consistent with independent biophysical data that characterise processes relevant to regulation of *lac* expression. Although phenomenological models were developed to reproduce the steady-state

behaviour [2] and the experimentally characterised dynamics of switching between stable steady states [11], these models were not constrained by independent biophysical data. For example, it is unclear whether the phenomenological models are consistent with independently measured permease transport kinetics. On the other hand, studies of bistability using more detailed, biophysical models of *lac* induction were either only partially constrained [7] or did not consider the response to artificial inducers [5, 6, 10].

Here we analyse bistability in ordinary differential equation (ODE) models of *lac* induction. We use ODEs because we restrict our analysis to steady-state behaviours, and because the protein concentrations in fully induced cells are $O(10^4)$ per cell (see Parameter Values section) and have negligible fluctuations. Similar equations describe induction by artificial inducers or lactose; however, the models for the two types of inducers are topologically distinct and one cannot be obtained as a limiting case of the other. We first use the artificial induction model to gain insight into key determinants of bistability of *lac* expression in response to TMG, and to understand how characteristics of bistability are controlled by model parameters. We then use the resulting insight to tune the parameters of the model to match the bistable behaviour observed by Ozbudak *et al.* [2], and to predict mechanisms by which bistability might be abolished. Finally, like previous modelling studies, we use the closely related lactose induction model to address the question of whether *lac* expression might be bistable in a natural context, contributing to resolution of what is now a long-standing controversy.

In our model of *lac* induction (Fig. 1a), the following set of coupled ordinary differential equations relate the internal lactose concentration (l), allolactose concentration (a) and β -galactosidase concentration (z) to the external lactose concentration (l^*)

$$\dot{l} = \alpha_0(l^* - l) + \alpha z \frac{(l^* - \phi \rho l)}{K_i + l^* + \rho l} - \frac{\beta z l / K_{m,l}}{1 + a/K_{m,a} + l/K_{m,l}} - \gamma l \quad (1a)$$

$$\dot{a} = \frac{\nu \beta z l / K_{m,l}}{1 + a/K_{m,a} + l/K_{m,l}} - \frac{\delta z a / K_{m,a}}{1 + l/K_{m,l} + a/K_{m,a}} - \gamma a \quad (1b)$$

$$\dot{z} = c\gamma + \frac{\epsilon \gamma a^n}{K_z^n + a^n} - \gamma z \quad (1c)$$

In (1), α and K_i are the rate constant and Michaelis constant for permease-dependent lactose import, $\phi\alpha$ and $\rho^{-1}K_i$ the rate constants for permease-dependent lactose export, β and $K_{m,l}$ the rate constant and Michaelis constant for lactose degradation, ν the branching fraction of lactose degradation to allolactose, δ and $K_{m,a}$ the rate constant and Michaelis constant for allolactose degradation, γ the rate of dilution due to cell growth, $c\gamma$ and $\epsilon\gamma$ the basal and inducible rates of β -galactosidase production, K_z the

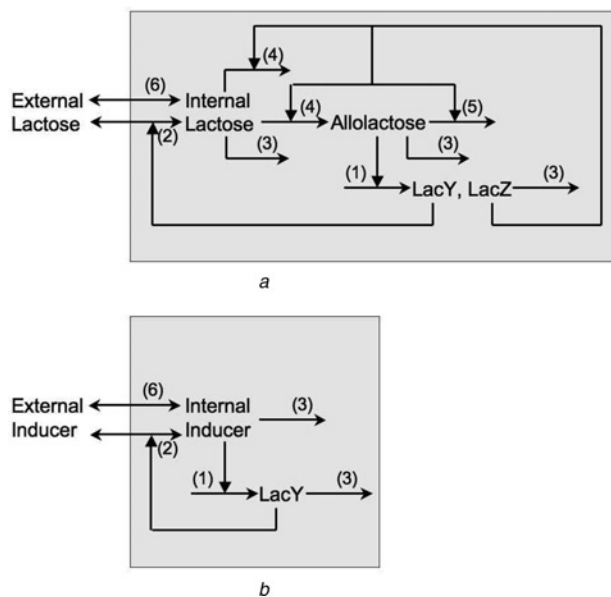


Figure 1 Circuitry for models of lac induction

a Model for induction by lactose (1), including the following processes:

1. Proportional production of permease (LacY) and β -gal (LacZ)
2. Permease-mediated transport of lactose
3. Dilution of intracellular species by cell growth
4. β -gal catalysed degradation of lactose, producing both the metabolic intermediate allolactose, and the ultimate products of degradation, glucose and galactose
5. β -gal catalysed degradation of allolactose, producing glucose and galactose
6. Passive transport of inducer

b Model for induction by artificial inducers (2), including:

1. Proportional production of permease (LacY) and β -gal (LacZ)
2. Permease-mediated transport of inducer
3. Dilution of intracellular species by cell growth
6. Passive transport of inducer

allolactose concentration at half-maximal induction of β -galactosidase production and n the Hill number for lactose induction of β -galactosidase production. The metabolic fluxes in (1) include the effects of competition between allolactose and lactose for access to β -galactosidase (β and δ terms).

The model of permease-dependent transport (α term) is consistent with the kinetic scheme described in [12], in which permease switches between inward- and outward-binding conformations, and accepts substrate from either the interior or exterior of the cell depending on the conformation. Active transport ($\phi < 1$) occurs through co-transport of substrate with a proton (symport), and is powered by a proton gradient across the membrane. The transport model is supported by crystallography studies [13, 14]. Changes in interior and exterior pH, membrane potential and the equilibrium constant between inward- and outward-facing conformations are considered implicitly through changes in kinetic parameters; we assume these conditions are not influenced by changes in substrate concentration. We note that Lolkema *et al.* [12] considered

a limiting case (exchange) in which switching between the two conformations is only kinetically accessible when substrate is bound to the permease, and both active transport and efflux are blocked. Here we consider more general equations in which all transitions in the model are allowed; our transport equation therefore differs from that in [12].

To focus on the operating conditions of the system that are most relevant to lactose utilisation by *E. coli*, we only consider regulation in the absence of glucose. This focus is appropriate because, in the presence of glucose, *lac* is not essential for growth, and induced β -galactosidase levels are low [15].

The model of artificial induction of *lac* (Fig. 1*b*) is given by

$$\dot{l} = \alpha_0(l^* - l) + \alpha z \frac{(l^* - \phi \rho l)}{K_i + l^* + \rho l} - \gamma l \quad (2a)$$

$$\dot{z} = c\gamma + \frac{\epsilon \gamma l^n}{K_z^n + l^n} - \gamma z \quad (2b)$$

In (2), variables and parameters have the same meaning as in (1), except l and l^* correspond to the level of internal and external artificial inducer (e.g. IPTG or TMG), respectively, and α_0 is the rate constant for permease-independent passive transport across the membrane.

In (1) and (2), protein expression is lumped with gene expression, and the dependence of promoter activity on the level of signal (TMG or allolactose) is modelled using a simple Hill function, which is significantly simpler than other models [5–10, 16, 17]. On the other hand, (1) considers the effects of competition among substrates in permease transport and metabolic processes, unlike other models of *lac* induction [2–7, 9, 10, 16, 18]. Compared with the model of Savageau [3, 4], (1) considers operon-independent decay of allolactose, without which bistability in response to lactose is impossible [3, 4, 7], as discussed above. Overall, (1) and (2) are less detailed than the *lac* induction models used in [5–7, 9, 10, 16] and are more detailed than those used in [2–4, 18] and they therefore constitute intermediate complexity equations describing *lac* induction. Compared with the simpler models, the intermediate level of detail provides increased contact between model parameters and biophysical measurements, and compared with more detailed models, it facilitates analysis of the equations and interpretation of the results.

2 Parameter values

We used the parameter values and ranges listed in Table 1 to analyse bistability in (1) and (2). The values in the table were obtained as follows:

- γ . We assume the doubling time under the conditions described in [2] is 30–60 min. We note, however, that this

Table 1 Parameter values

Parameter	Description	Nominal	Range
γ	growth rate	—	$0.0116\text{--}0.0231\text{ min}^{-1}$
α_0	passive transport rate constant	0	$0\text{--}1.35\text{ min}^{-1}$
α	permease import turnover number	600 min^{-1}	$6 \times 10^1\text{--}6 \times 10^3\text{ min}^{-1}$
ϕ	ratio of permease export-to-import turnover numbers	0.5	0–0.5
K_i	permease Michaelis constant	$5 \times 10^5\text{ nM}$	$5 \times 10^4\text{--}5 \times 10^6\text{ nM}$
ρ	ratio of permease import-to-export Michaelis constants	0.1	0.1–1
β	β -gal lactose turnover number	$2.85 \times 10^4\text{ min}^{-1}$	$2.85 \times 10^3\text{--}2.85 \times 10^5\text{ min}^{-1}$
ν	lactose \rightarrow allolactose β -gal branching fraction	0.468	—
$K_{m,l}$	β -gal lactose Michaelis constant	2.53 mM	0.253–25.3 mM
δ	β -gal allolactose turnover number	$2.30 \times 10^4\text{ min}^{-1}$	$2.30 \times 10^3\text{--}2.30 \times 10^5\text{ min}^{-1}$
$K_{m,a}$	β -gal allolactose Michaelis constant	1.2 mM	0.12–12.0 mM
ϵ	fully induced β -gal level	34 286 nM	—
c	basal β -gal level	34.3 nM	—
K_z	signal level at half-maximal <i>lac</i> induction	10^5 nM	$10^4\text{--}10^6\text{ nM}$
n	Hill number for signal-dependent <i>lac</i> induction	2	—

Nominal values are those used to generate the lactose induction curves in Fig. 8

time might be very different for *E. coli* growing under stress in the gut or aqueous environment; this represents a source of uncertainty concerning the biological relevance of our predictions.

- α_0 . Experimental data on passive transport of inducers seem scarce in the literature. Maloney and Wilson [19] report a measured rate constant of 0.14 min^{-1} for TMG, and Kepes [20] reports permease-independent efflux rate constants of 0.022 and 0.054 min^{-1} for lactose measured under conditions of deinduction and induction, respectively. However, the TMG value was obtained using competitive inhibition of permease using an undescribed method, and the lactose values were obtained using a model of lactose flux that is inconsistent with the mechanism provided in [12], and that ignores dilution by cell growth. We therefore consider the above values to be uncertain. Here we explore the same range as that used in the modelling study described in [9], which encompasses the above values. We analyse the lactose system using a nominal value of 0, allowing for the possibility that the actual value might be very small; this value also maximises the potential for bistability.

- α . An approximate range of $1\text{--}100\text{ s}^{-1}$ for sugar transport turnover numbers was obtained from the review by Wright *et al.* [21]. The range is broader than measured values [22] because measurements were made at 25°C rather than at the physiological temperature of 37°C in the host environment of the gut, and at which measurements in [2]

were performed. Turnover numbers can vary by about an order of magnitude depending on the membrane potential and proton gradient [22], leading to additional uncertainty. The nominal value of 600 min^{-1} is consistent with that in [22] assuming the production rate of functional permease is about the same as that of functional β -gal. Because permease is a monomer while β -gal is a tetramer, this assumption entails a four-fold smaller synthesis rate for permease monomers compared with β -gal subunits. This seems possible, as (i) galactoside acetyltransferase (GATase) monomer synthesis is eight-fold smaller than β -gal subunit synthesis; (ii) due to incomplete operon transcription and the order of genes in the operon (*lacZYA*), the amount of mRNA transcribed from the GATase gene (*lacA*) and permease gene (*lacY*) is smaller than that from the β -gal gene (*lacZ*); (iii) there is some evidence that permease monomers are made in smaller amounts than β -gal subunits [23].

- ϕ . The nominal value of 0.5 was obtained by comparing the active transport and efflux turnover numbers in Viitanen *et al.* ([22] Table 1). Because permease transport kinetics are sensitive to membrane potential and proton gradient [22], we allow the value to decrease in the search for bistable conditions (we found that bistability is abolished for higher values of ϕ).

- K_i . A nominal value of 0.5 mM was obtained from Ref. [22]. The range was applied as per α and encompasses measured values [22, 24, 25].

- ρ . Guided by Viitanen *et al.* ([22], Table 1), we assume that the Michaelis constant for permease-dependent import can be up to 10 times smaller than that for export. The nominal value of 0.1 is consistent with the smallest in that table, and yields the greatest potential for bistability in the lactose system.

- β . A total lactose turnover number for β -galactosidase of $2.85 \times 10^4 \text{ min}^{-1}$ is estimated from a measured value of $V_{\max} = 61.3 \mu\text{M min}^{-1} \text{ mg}^{-1}$ in [27]. This estimate is an order of magnitude greater than the value $3.6 \times 10^3 \text{ min}^{-1}$ given in [27], but the two estimates agree closely when one considers that β -gal converts about half of its lactose substrate to glucose and galactose, rather than allolactose, and that the enzyme is composed of four monomeric catalytic subunits. The estimate given in [27] is appropriate for total turnover of lactose on a per monomer basis. Like for α , because measurements were performed at 30°C , we consider a range of values 10 times lower to 10 times higher than the nominal value.

- $K_{m,l}$. The nominal value was obtained directly from Huber *et al.* [28]. As for β , because of temperature considerations, we use a range from 10 times lower to 10 times higher than the nominal value.

- ν . The value $\nu = 0.468$ was calculated from the total rate of β -gal degradation of lactose and the partial flux from lactose to allolactose reported in [26]. We take it to be a constant because the ratio of reaction products was found to be insensitive to temperature changes between 30°C and 0°C .

- δ . An allolactose turnover number for β -gal of $2.3 \times 10^4 \text{ min}^{-1}$ is estimated from a measured value of $V_{\max} = 49.6 \mu\text{mol min}^{-1} \text{ mg}^{-1}$ in [28]. As for β , because of temperature considerations, we use a range from 10 times lower to 10 times higher than the nominal value.

- $K_{m,a}$. The nominal value was obtained directly from Huber *et al.* [28]. As for β , because of temperature considerations, we use a range from 10 times lower to 10 times higher than the nominal value.

- ϵ . Using a production rate of five β -gal tetramers per cell per second for a 48 min generation time [29], 14 400 molecules are produced during a generation at full induction – this is the number of molecules in the cell after doubling (supporting our choice of a noiseless model). Assuming a $1 \mu\text{m}^3$ mean cell volume [30] and linear volume increase in time [31], the volume after doubling is $\sim 0.7 \mu\text{m}^3$, leading to a concentration of 34 286 nM.

- c . This value is derived from ϵ , assuming a 1000-fold increase in β -galactosidase levels upon induction [32].

- K_z and n . These values are estimated from IPTG induction data in permease knockout cells both from Sadler

and Novick ([33], Fig. 15) and from data compiled by Yagil and Yagil ([34], Figs. 1 and 2). The nominal value $n = 2$ was estimated from the slopes of the curves in the figures, and K_z was determined by estimating from the figures the concentration of IPTG at half-maximal induction. The nominal value of 10^5 nM was estimated from *lac* induction data in [33] and [34]. We allowed for a range from 10^4 nM to 10^6 nM to account for potential differences between induction by IPTG and TMG or lactose.

3 Results

We first used (2) to determine how parameter values control bistability in the steady-state response of *lac* expression to artificial inducers. To detect and characterise bistability for a given set of parameter values, we solved for $z(l)$ and $l^*(l)$ as rational functions of l . Bistability in *lac* expression exists when the line describing steady-state levels of z against l^* adopts a characteristic 'S' shape, as shown in Fig. 2. Within the bistable range of l^* , the highest and lowest levels of z are stable steady-state solutions and the intermediate level of z is an unstable steady-state solution of (1). The bistable range is defined by the lower ($l^* = L$) and upper ($l^* = U$) turning points, as illustrated in Fig. 2. An analogous signature of bistability can be seen in examining steady-state levels of l against l^* (not shown). For a model with given parameter values, L and U can be located by finding the roots of either dl^*/dz or dl^*/dl using an eigenvalue solver.

We analysed (2) for systems with $\alpha_0 = 0$ and $\phi = 0$, $\rho = 1$, $n = 2$ and all other sets of parameter values drawn

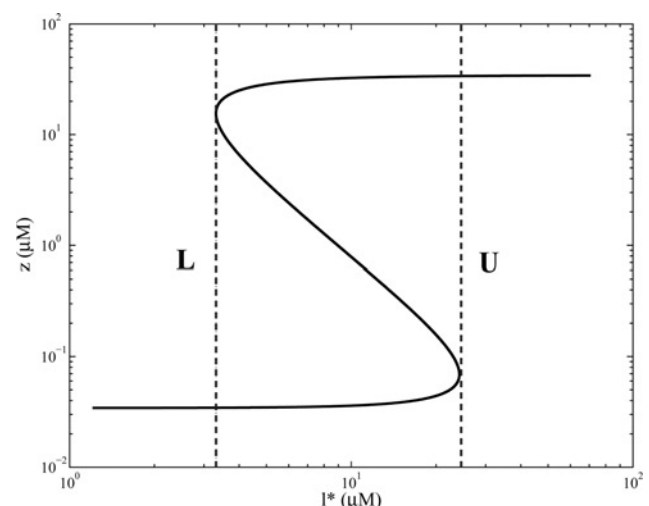


Figure 2 Example of bistable behaviour in the artificial induction model (2)

The upper (U) and lower (L) turning points are consistent with the experimental results in [2]

The parameter values are $\gamma = 0.0231 \text{ min}^{-1}$, $\alpha = 60 \text{ min}^{-1}$, $K_z = 123\,285 \text{ nM}$ and $K_l = 1\,077\,217 \text{ nM}$

from the ranges in Table 1. Sets of 100 values each for K_i and K_z were obtained using logarithmically even sampling over their allowed ranges. Because the steady-state solutions of (2) only depend on α and γ through the ratio α/γ , rather than sampling α and γ individually, we obtained 100 values of α/γ using logarithmically even sampling between the upper- and lower-bound computed from Table 1. This sampling scheme yielded $100 \times 100 \times 100 = 10^6$ systems with different values of $(\alpha/\gamma, K_i, K_z)$.

We found that all 10^6 systems exhibited some degree of bistability in response to induction by artificial inducers. The dependence of the range of bistability on model parameters was further analysed using two measures that we introduce here: the ratio U/L and the product UL . We used these measures to estimate the percentage of systems for which bistability might be observable in an experiment such as that in [2]. By inspecting the measurement errors in [2], we estimate that systems with $U/L > 1.1$ and $UL > 0.01 \mu\text{M}^2$ exhibit bistability that is favourable for experimental observation, and that systems with either $U/L < 1.1$ or $UL < 0.01 \mu\text{M}^2$ exhibit bistability that is unfavourable for experimental observation. Among systems with parameter values sampled as described above, by these criteria, experimental observation of bistability is favourable for 65% of systems, and unfavourable for 35% of systems.

To compare (2) with the data in [2], we first selected a subset of systems for which the bistable region is in the same neighbourhood as that in [2]: from 3 to 30 μM TMG. Considering this range, out of the 10^6 systems sampled, we selected 187 108 systems for which $L > 1 \mu\text{M}$ and $U < 100 \mu\text{M}$ for further analysis. Interestingly, we found that all of these systems collapse to a single curve when displayed in the space of $\log_{10}(U/L)$ against $\log_{10}(K_i/K_z)$ (Fig. 3), indicating that U/L can be precisely tuned using the parameter $X = K_i/K_z$. As shown in Fig. 3, the dependence was accurately modelled using the equation

$$\log_{10}(U/L) \simeq \frac{(K_i/K_z)^{0.93}}{(K_i/K_z)^{0.93} + (0.27)^{0.93}} - \frac{1}{10} \geq 0 \quad (3)$$

Next, we found that, at a given value of $X = K_i/K_z$, without changing the value of U/L , UL could be tuned precisely using the parameter $Y = K_i K_z \gamma / \alpha$. As shown in Fig. 4, this dependence was accurately modelled using the equation

$$\log_{10}(UL) = C_0(X) + C_1(X) \log_{10}(Y) \quad (4)$$

Fig. 5 shows the X -dependence of the parameters $C_0(X)$ and $C_1(X)$, obtained numerically using systems with similar values of X . For the range of systems considered here, we found that $C_0(X)$ could be fit using a third-order polynomial in $\log_{10}(X)$, and that $C_1(X)$ could be taken as a constant.

We used (3) and (4) to obtain a family of systems that are consistent with the parameter values in Table 1 and that exhibit a range of bistability consistent with that observed

in [2], with $\log_{10}(U/L) \simeq 0.86$ and $\log_{10}(UL) \simeq 1.92$. An example of the steady-state behaviour of one such system is illustrated in Fig. 2.

Increasing either α_0 or ϕ above zero tends to reduce or abolish bistability in artificially induced systems. As α_0 is increased (Fig. 6), first U begins shifting to lower values of l^* , then L begins shifting to higher values of l^* , leading to

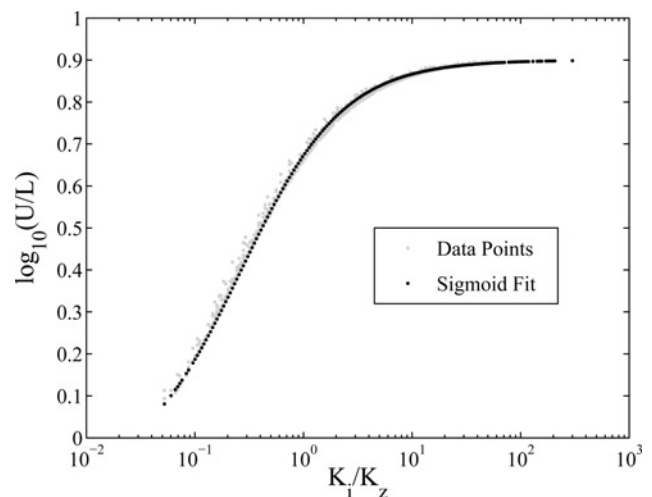


Figure 3 Relation between U/L and the parameter $X = K_i/K_z$

Data points are generated using the artificial induction model (2) with parameter values selected as described in the text. Points with $L > 1 \mu\text{M}$ and $U < 100 \mu\text{M}$ were selected; shown are a subset of points that illustrate the general trend, which is well described using (3).

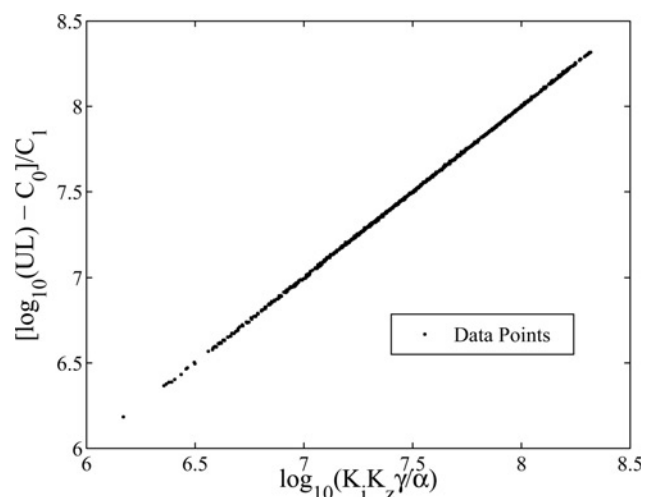


Figure 4 Relation between the bistability measure UL and the parameter $Y = K_i K_z \gamma / \alpha$

Using the coefficients C_0 and C_1 (Fig. 5) as indicated on the y -axis yields a linear relation that is well-modelled using (4). The data points are generated as described in Fig. 3 and in the text.

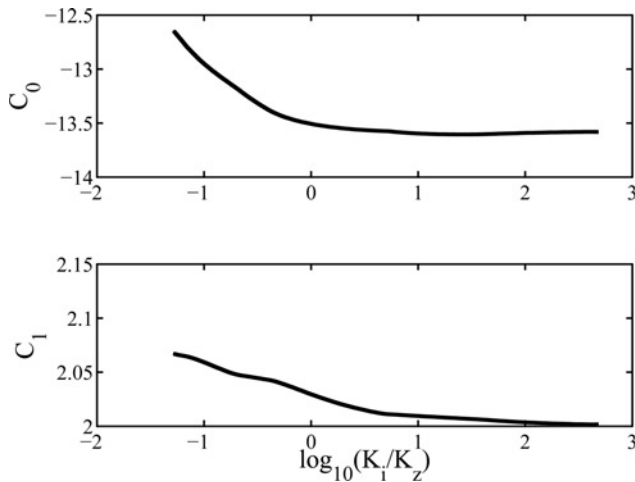


Figure 5 Dependence of the coefficients for the UL regression model in (4) on $X = K_i/K_z$

By allowing C_0 and C_1 to depend on X , the bistability measure UL has a simple linear relationship with $Y = K_i K_z \gamma / \alpha$ (Fig. 4). The value of X is determined by (3) for a given value of U/L (Fig. 3).

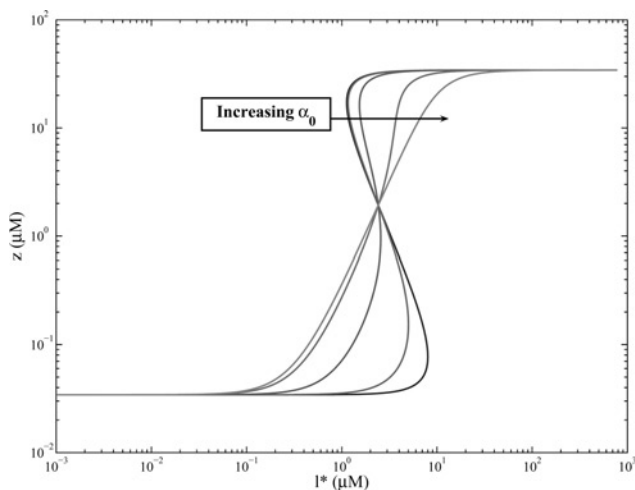


Figure 6 Effects of variations in the $\alpha_0 > 0$ parameter on an artificially induced system with $\phi = 0 \text{ min}^{-1}$ and $\alpha_0 = 10^{-k} \text{ min}^{-1}$, $k = 0, \dots, 4$

The other parameters are given by $n = 2$, $\gamma = 0.0231 \text{ min}^{-1}$, $\epsilon = 34.286 \text{ nM}$, $c = 34.3 \text{ nM}$, $K_i = 5 \times 10^6 \text{ nM}$, $K_z = 10^4 \text{ nM}$ and $\alpha = 60 \text{ min}^{-1}$.

an asymptotic behaviour in which bistability is abolished. Like changes in α_0 , as ϕ is increased (Fig. 7), L shifts to higher values of l^* ; however, in contrast, U does not initially show a significant change. As ϕ is increased further, the entire induction curve begins to shift to higher levels of l^* .

We then considered systems with $\rho < 1$. Using (2), we found that the steady-state behaviour of such systems is equivalent to that of systems with $\rho = 1$ under the

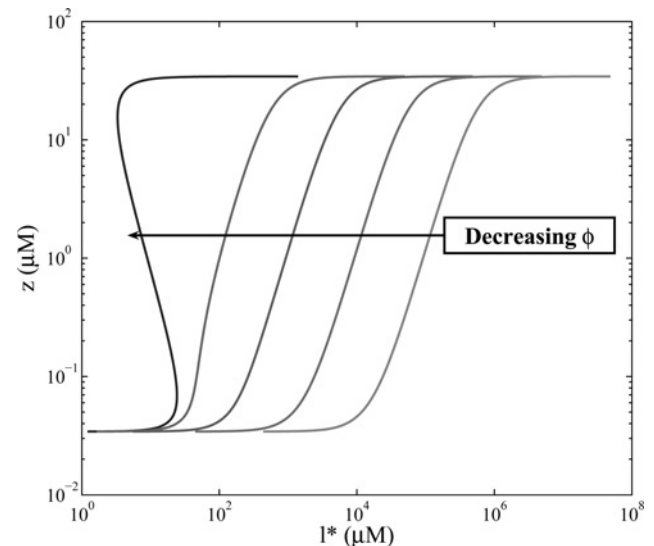


Figure 7 Effects of variations in the $\phi > 0$ parameter on an artificially induced system with $\alpha_0 = 10^{-4} \text{ min}^{-1}$ and $\phi = 0$ and 10^{-k} min^{-1} , $k = 1, \dots, 4$

The other parameter values are as in Fig. 6

transformation

$$l \rightarrow \rho l \quad (5a)$$

$$K_z \rightarrow \rho K_z \quad (5b)$$

$$\gamma \rightarrow \frac{\gamma}{\rho} + (1 - \rho) \frac{\alpha_0}{\rho} \quad (5c)$$

Because both K_i/K_z and $K_i K_z \gamma / \alpha$ increase under this transformation, we expected bistability to be enhanced in systems with $\rho < 1$ (Figs. 3 and 4). Indeed, we found that bistability in systems with $\rho < 1$ exhibited a higher tolerance to increases in α_0 and ϕ : for example, the system with $K_z = 10 \text{ uM}$, $K_i = 5 \text{ mM}$, $\alpha = 890 \text{ min}^{-1}$, $\phi = 0.1$, $\alpha_0 = 10^{-3} \text{ min}^{-1}$ and $\rho = 0.1$ exhibits bistability with $\log_{10}(U/L) = 0.85$ and $\log_{10}(UL) = 1.91$, which is consistent with the data in [2].

We used similar methods to analyse (1) which describes induction by lactose. Like the artificial induction model, the steady-state behaviour of systems with $\rho < 1$ is equivalent to that of systems with $\rho = 1$ under the transformations in (5), with the additional re-scaling

$$K_{m,l} \rightarrow \rho K_{m,l} \quad (6)$$

No bistability was present in the system with nominal parameter values from Table 1 with $\phi = 0.5$ (Fig. 8), which is consistent with the theory of Savageau [3] and the Supplementary Material of Ozbudak *et al.* [2]. However, guided by the results for artificial inducers in Fig. 7, we examined systems with $\phi = 0$. Although the system with otherwise nominal parameter values did not exhibit bistability, other systems that have parameter values consistent with the ranges in Table 1 did exhibit bistability.

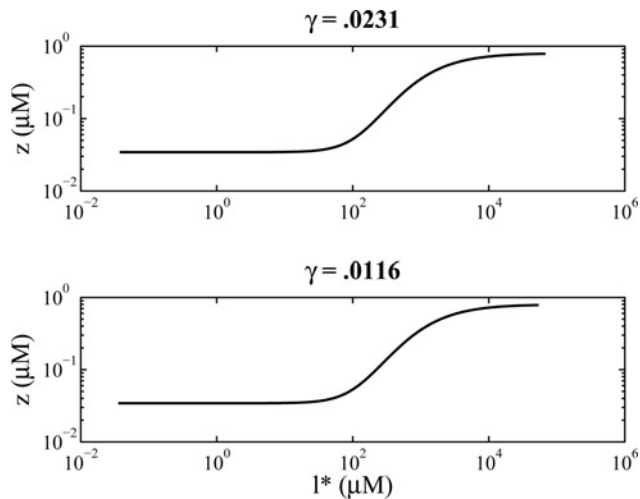


Figure 8 Lactose induction behaviour calculated using the nominal values in Table 1

Neither the system with $\gamma = 0.231 \text{ min}^{-1}$ (top) nor the system with $\gamma = 0.116 \text{ min}^{-1}$ (bottom) exhibits bistability

We located the system that exhibits the largest values of U/L and UL ; for this case, α , β , δ , ρ and K_z assume their lowest values in Table 1 while γ , $K_{m,l}$, $K_{m,a}$ and K_i assume their highest values (Fig. 9).

To estimate the distribution of systems exhibiting the different qualitative behaviours, as for the case of artificial inducers, we analysed 10^5 systems with randomly sampled parameter values, all with $\phi = 0$ and $\rho = 0.1$. We found that 99.82% of these systems exhibits no bistability, 0.07% exhibit bistability favourable for observation ($U/L > 1.1$ and $UL > 0.01 \mu\text{M}^2$), and 0.11% to exhibit bistability that is unfavourable for observation ($U/L < 1.1$ or $UL < 0.01 \mu\text{M}^2$). These statistics are virtually unchanged

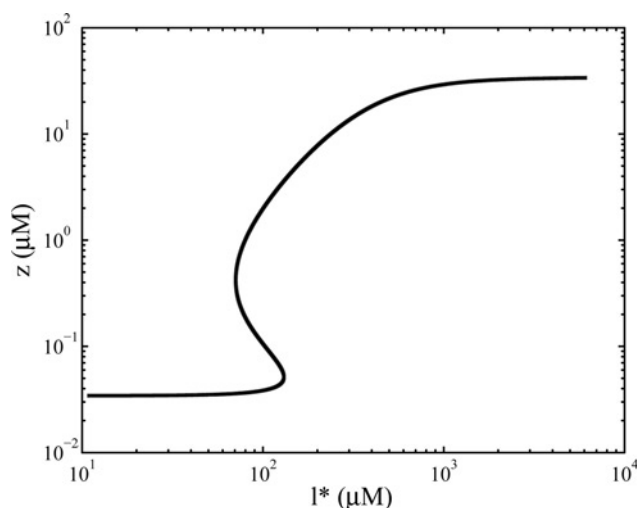


Figure 9 Bistability in the $\phi = 0$ lactose-induced system with α , β , δ , ρ and K_z at their lowest values in Table 1 and γ , $K_{m,l}$, $K_{m,a}$ and K_i at their highest values

This is the system that exhibits the largest values of U/L and UL within the allowed ranges of parameter values

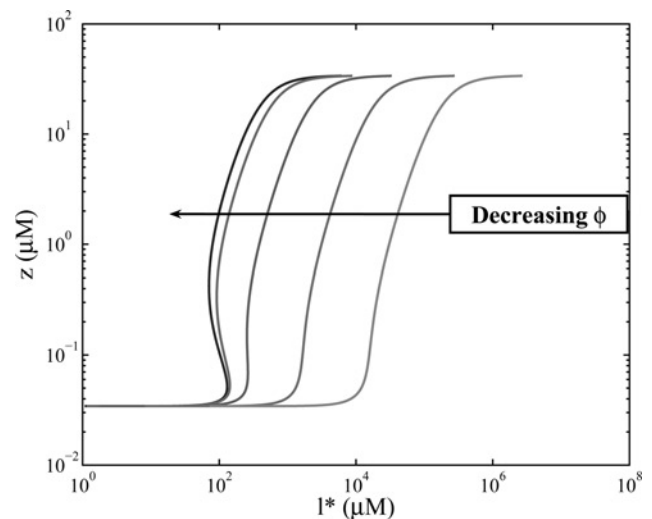


Figure 10 Influence of ϕ on bistability in lactose induction

Leftmost curve corresponds to the same system illustrated in Fig. 9, except with $\rho = 1$ (the two are nearly identical)

Curves to the right correspond to the same systems, except $\phi = 10^{-k} \text{ min}^{-1}$, $k = 1, \dots, 4$

Bistability in lactose induction is abolished even for small values of ϕ

for systems with $\rho = 1$. Increasing ϕ to even a small fraction of its nominal value rapidly abolishes bistability for all combinations of other parameter values in (1) (Fig. 10).

4 Discussion

For the equations describing induction by artificial inducers, we found that the range of external inducer concentrations over which systems with $\alpha_0 = 0$ and $\phi = 0$ exhibit bistability is precisely controllable by two rational combinations of model parameters. First, the value of U/L can be specified by choosing a value of the parameter $X = K_i/K_z$ using (3). Then, using this value of X , the value of UL can be specified by choosing a value of the parameter $Y = K_z K_i \alpha / \gamma$ using (4) and the empirically determined $C_0(X)$ and $C_1(X)$ (Fig. 5). By adjusting these parameters, we were able to demonstrate agreement with the bistable range for TMG induction from Ozbudak *et al.* [2].

Small increases in α_0 and ϕ abolished bistability in artificially induced systems with $\rho = 1$. Bistability was less sensitive to increases in α_0 and ϕ in systems with $\rho = 0.1$; however, even with $\rho = 0.1$, bistability was abolished in systems with α_0 as high as 0.01 min^{-1} . This value is smaller than measured permease-independent diffusion rates for TMG [19] and lactose [20]; combined with uncertainty in these measurements (Parameter values), this discrepancy motivates further studies of permease-independent diffusion of *lac* inducers.

To achieve agreement with the bistable range of $\sim 3\text{--}30 \mu\text{M}$ in [2], c and ϵ in (2) were tuned to exhibit a 1000-fold induction of protein expression. While

this value is reasonable based on previous studies, at first glance, it appears to disagree with the ~ 100 -fold induction of GFP expression reported in [2]. Indeed, we analysed systems with alternative values of ϵ and ϵ' that yield 100-fold induction, and none of them exhibited bistable ranges that agree with the range reported in [2]. However, the *lac::gfp* reporter used in [2] begins at -84 with respect to the start site, and extends to $+20$; it therefore seems to be missing all of the O2 sequence, and some of the O3 sequence. Such a difference could easily lead to a 10-fold difference in induction of the reporter compared with the native *lac* promoter; evidence for such an effect could be sought experimentally, for example by calibrating the fluorescence levels against measurements of β -gal activity.

The curve in Fig. 9 illustrating an extreme example of bistability in response to lactose for $\phi = 0$ closely resembles a similar curve shown by van Hoek and Hogeweg ([7] Fig. 2b). Thus, although our model is less detailed than theirs, it can exhibit comparable steady-state behaviour. In addition, they [9] considered a stochastic model of *lac* induction, and Narang and Pilyugin [8] considered a more detailed model of the dependence of promoter activity on the level of inducer that includes DNA looping; nevertheless, like the present study, Refs. [7–9] each reported a lack of bistability in lactose induction of *lac*. These consistencies lend support to our choice of an intermediate complexity model of bistability in *lac*.

5 Conclusions

The lack of bistability observed for induction by lactose agrees with modelling studies concluding that bistability in *lac* expression is irrelevant to *E. coli* in a natural context [3, 4, 7–9]. Thus, although bistable behaviour in *lac* is now well-documented [1, 2, 35], because it has only been experimentally observed using artificial inducers, its relevance within the natural context of *E. coli* is doubtful. Indeed, it is surprising that the *lac* operon has been considered to be a paradigm of bistability in gene regulation, considering the gaps in understanding that remain after so many careful experimental and theoretical studies.

The present results predict that bistable behaviour can be promoted by (i) hindering the kinetics of permease transport (α , K_i) and β -gal catalysis (β , δ , $K_{m,l}$, $K_{m,a}$); (ii) lowering the required level of allolactose for half-maximal *lac* expression (K_z); (iii) accelerating cell growth (γ); and (iv) decreasing the Michaelis constant for permease influx relative to that for efflux (ρ). These predictions suggest genetic targets for engineering *E. coli* strains that exhibit a clear signature of bistability. Experiments to compare the behaviour of such strains with wild-type cells would help to clarify whether bistability in *lac* expression is relevant in a natural context.

Here, we found that metabolic fluxes are key determinants of bistability in *lac* induction, and that the qualitative behaviour of the system can change depending on the metabolism of inducers. Previously, we found that diversity in the interaction of an input signal with transcription factors leads to diversity in the qualitative behaviour of a feed-forward loop gene circuit [36]. We expect these findings to apply broadly to genetic regulatory systems in *E. coli* and other organisms. Overall, the results of these studies emphasise the importance of the nature of the input signal in determining the functions of genetic regulatory circuits.

6 Acknowledgment

We thank Michael A. Savageau for discussions, and Atul Narang for reading the manuscript. This work was supported by the US Department of Energy through contract DE-AC52-06NA25396, and grant GM 80216 from the National Institutes of Health. The collaboration was facilitated by the First q-bio Summer School on Cellular Information Processing, which was sponsored by the New Mexico Consortium's Institute for Advanced Studies, and the Center for Nonlinear Studies at Los Alamos National Laboratory.

7 References

- [1] NOVICK A., WEINER M.: 'Enzyme induction as an all-or-none phenomenon', *Proc. Natl. Acad. Sci. USA*, 1957, **43**, pp. 553–566
- [2] OZBUDAK E.M., THATTAI M., LIM H.N., SHRAIMAN B.I., VAN OUDENAARDEN A.: 'Multistability in the lactose utilization network of *Escherichia coli*', *Nature*, 2004, **427**, (6976), pp. 737–740
- [3] SAVAGEAU M.A.: 'Design principles for elementary gene circuits: Elements, methods, and examples', *Chaos*, 2001, **11**, (1), pp. 142–159
- [4] SAVAGEAU M.A.: 'Alternative designs for a genetic switch: analysis of switching times using the piecewise power-law representation', *Math. Biosci.*, 2002, **180**, pp. 237–253
- [5] YILDIRIM N., MACKEY M.C.: 'Feedback regulation in the lactose operon: a mathematical modelling study and comparison with experimental data', *Biophys. J.*, 2003, **84**, (5), pp. 2841–2851
- [6] YILDIRIM N., SANTILLAN M., HORIKE D., MACKEY M.C.: 'Dynamics and bistability in a reduced model of the *lac* operon', *Chaos*, 2004, **14**, (2), pp. 279–292
- [7] VAN HOEK M.J., HOGEWEG P.: 'In silico evolved *lac* operons exhibit bistability for artificial inducers, but not for lactose', *Biophys. J.*, 2006, **91**, (8), pp. 2833–2843

- [8] NARANG A., PILYUGIN S.S.: 'Bistability of the *lac* operon during growth of *Escherichia coli* on lactose and lactose + glucose', *Bull. Math. Biol.*, 2008, **70**, (4), pp. 1032–1064
- [9] VAN HOEK M., HOGEWEG P.: 'The effect of stochasticity on the *lac* operon: an evolutionary perspective', *PLoS Comput. Biol.*, 2007, **3**, (6), p. e111
- [10] SANTILLAN M., MACKEY M.C., ZERON E.S.: 'Origin of bistability in the *lac* operon', *Biophys. J.*, 2007, **92**, (11), pp. 3830–3842
- [11] METTETAL J.T., MUZZEY D., PEDRAZA J.M., OZBUDAK E.M., VAN OUDENAARDEN A.: 'Predicting stochastic gene expression dynamics in single cells', *Proc. Natl. Acad. Sci. USA*, 2006, **103**, pp. 7304–7309
- [12] LOKKEMA J.S., CARRASCO N., KABACK H.R.: 'Kinetic analysis of lactose exchange in proteoliposomes reconstituted with purified *lac* permease', *Biochemistry*, 1991, **30**, (5), pp. 1284–1290
- [13] ABRAMSON J., SMIRNOVA I., KASHO V., VERNER G., KABACK H.R., IWATA S.: 'Structure and mechanism 22 of the lactose permease of *Escherichia coli*', *Science*, 2003, **301**, (5633), pp. 610–615
- [14] GUAN L., MIRZA O., VERNER G., IWATA S., KABACK H.R.: 'Structural determination of wild-type lactose permease', *Proc. Natl. Acad. Sci. USA*, 2007, **104**, (39), pp. 15294–15298
- [15] MAGASANI B., NEIDHARDT F.C.: 'Regulation of carbon and nitrogen utilization', in NEIDHARDT F.C. (ED.): 'Escherichia coli and Salmonella typhimurium: cellular and molecular biology' (American Society for Microbiology, Washington, DC, 1987, vol. 2, 1st edn.), pp. 1318–1325
- [16] WONG P., GLADNEY S., KEASLING J.D.: 'Mathematical model of the *lac* operon: inducer exclusion, catabolite repression, and diauxic growth on glucose and lactose', *Biotechnol. Prog.*, 1997, **13**, (2), pp. 132–143
- [17] NARANG A.: 'Effect of dna looping on the induction kinetics of the *lac* operon', *J. Theor. Biol.*, 2007, **247**, (4), pp. 695–712
- [18] VILAR J.M., GUET C.C., LEIBLER S.: 'Modeling network dynamics: the *lac* operon, a case study', *J. Cell Biol.*, 2003, **161**, (3), pp. 471–476
- [19] MALONEY P.C., WILSON T.H.: 'Quantitative aspects of active transport by the lactose transport system of *Escherichia coli*', *Biochim. Biophys. Acta*, 1973, **330**, (2), pp. 196–205
- [20] KEPES F.: 'M'ecanismes d'efflux d'un substrat accumul'e par la lactose perm'ease de *Escherichia coli*: 'etude th'eorique et exp'erimentale', *Biochimie*, 1985, **67**, (1), pp. 69–73
- [21] WRIGHT J.K., SECKLER R., OVERATH P.: 'Molecular aspects of sugar:ion cotransport', *Annu. Rev. Biochem.*, 1986, **55**, pp. 225–248
- [22] VIITANEN P., GARCIA M.L., KABACK H.R.: 'Purified reconstituted *lac* carrier protein from *Escherichia coli* is fully functional', *Proc. Natl. Acad. Sci. USA*, 1984, **81**, (6), pp. 1629–1633
- [23] KENNEDY E.P.: 'The lactose permease system of *E. coli*', in BECKWITH J.R., ZIPSER D. (EDS.): 'The lactose operon' (Cold Spring Harbor Laboratory, Cold Spring Harbor, NY, 1970), pp. 49–92
- [24] WRIGHT J.K., RIEDE I., OVERATH P.: 'Lactose carrier protein of *Escherichia coli*: interaction with galactosides and protons', *Biochemistry*, 1981, **20**, (22), pp. 6404–6415
- [25] PAGE M.G., WEST I.C.: 'The transient kinetics of uptake of galactosides into *Escherichia coli*', *Biochem. J.*, 1984, **223**, (3), pp. 723–731
- [26] HUBER R.E., KURZ G., WALLENFELS K.: 'A quantitation of the factors which affect the hydrolase and transgalactosylase activities of beta-galactosidase (*E. coli*) on lactose', *Biochemistry*, 1976, **15**, (9), pp. 1994–2001
- [27] MARTINEZ-BILBAO M., HOLDSWORTH R.E., EDWARDS L.A., HUBER R.E.: 'A highly reactive beta-23 galactosidase (*Escherichia coli*) resulting from a substitution of an aspartic acid for gly-794', *J. Biol. Chem.*, 1991, **266**, (8), pp. 4979–4986
- [28] HUBER R.E., WALLENFELS K., KURZ G.: 'The action of beta-galactosidase (*Escherichia coli*) on allolactose', *Can. J. Biochem.*, 1975, **53**, (9), pp. 1035–1038
- [29] KENNEL D., RIEZMAN H.: 'Transcription and translation initiation frequencies of the *Escherichia coli lac* operon', *J. Mol. Biol.*, 1977, **114**, (1), pp. 1–21
- [30] KUBITSCHKE H.E., FRISKE J.A.: 'Determination of bacterial cell volume with the coulter counter', *J. Bacteriol.*, 1986, **168**, (3), pp. 1466–1467
- [31] KUBITSCHKE H.E.: 'Cell volume increase in *Escherichia coli* after shifts to richer media', *J. Bacteriol.*, 1990, **172**, (1), pp. 94–101
- [32] BECKWITH J.: 'The lactose operon', in NEIDHARDT F.C. (ED.): 'Escherichia coli and Salmonella typhimurium: cellular and molecular biology' (American Society for Microbiology, Washington, DC, 1987, vol. 2, 1st edn.), pp. 1444–1452
- [33] SADLER J.R., NOVICK A.: 'The properties of repressor and the kinetics of its action', *J. Mol. Biol.*, 1965, **12**, pp. 305–327

[34] YAGIL G., YAGIL E.: 'On the relation between effector concentration and the rate of induced enzyme synthesis', *Biophys. J.*, 1971, **11**, (1), pp. 11–27

[35] COHN M., HORIBATA K.: 'Analysis of the differentiation and of the heterogeneity within a population of *Escherichia*

coli undergoing induced beta-galactosidase synthesis', *J. Bacteriol.*, 1959, **78**, pp. 613–623

[36] WALL M.E., DUNLOP M.J., HLAVACEK W.S.: 'Multiple functions of a feed-forward-loop gene circuit', *J. Mol. Biol.*, 2005, **349**, (3), pp. 501–514